Waste heat recovery from a heavy-duty natural gas engine by Organic Rankine Cycle

Antonio Mariani [1,*], *Biagio* Morrone[1], *Maria Vittoria* Prati [2] and *Andrea* Unich[1]

[1]Department of Engineering, Università degli studi della Campania «L. Vanvitelli», Italy
[2]Istituto Motori CNR, Italy

Abstract. Waste heat recovery can be a key solution for improving the efficiency of energy conversion systems. Organic Rankine Cycles (ORC) are a consolidated technology for achieving such target, ensuring good efficiencies and flexibility. ORC systems have been mainly adopted for stationary applications, where the limitations of layout, size and weight are not stringent. In road transportation propulsion systems, the integration between the powertrain and the ORC system is difficult but still possible. The authors investigated an ORC system bottoming a spark ignited internal combustion engine (ICE) powering a public transport bus. The bus, fuelled by natural gas, was tested in real driving conditions. Exhaust gas mass flow rate and temperature have been measured for calculating the thermal power to be recovered in the ORC plant. The waste heat was then used as energy input in a model simulating the performance of an ORC system. The heat transfer between the exhaust gases and the ORC fluid is crucial for the ORC performance. For this reason, attention was paid to considering the interaction between hot fluid temperature and ORC maximum pressure. ORC performance in terms of real cycle efficiency and power produced were calculated considering n-Pentane as working fluid. The fuel consumption was reduced from 271.5 g/km to 261.4 g/km over the driving cycle, corresponding to 3.7% reduction.

1 Introduction

The substitution of fossil fuels with renewable energy sources for power generation, heating and transportation requires time. Considering the actual economic scenario, characterized by low oil price, renewables are even less competitive. To reduce greenhouse gases [1] and pollutant emissions, it is thus fundamental to maximize the efficiency of the conversion systems. The transportation sector represents one third of the final energy consumption in the EU and almost 93% of such energy comes from oil [2]. The impact of transportation on the environment and health is critical in urban area. In fact, mobility in cities is largely based on passenger cars and buses, powered by fossil fuels. In public transport natural gas can replace diesel with advantages in terms of environmental impact and costs [3, 4].

* Corresponding author: antonio.mariani@unicampania.it

Internal combustion engine efficiency attains maximum values around 40% for diesel and the most advanced spark ignition engines, with lower values at part loads [5, 6], with heat rejected into the exhaust gases and the cooling system estimated to be 34–45% of the initial fuel energy in case of spark ignition (SI) engines and 22–35% for diesel engines [5]. This waste heat can be recovered into Organic Rankine Cycles (ORC) for additional power generation. According to the operating principle of Rankine cycles, the pressurized working fluid evaporates into an evaporator, expands delivering mechanical power and finally reverts to its initial state in a condenser.

ORC is a well-known technology but still recent for bottoming internal combustion engines due to the complexity of vehicle integration. Mass and size requirements, very stringent for passenger cars, are less relevant for marine propulsion [7], trucks and buses [8].

For minimizing ORC system weight, size and cost as well as for maximizing system efficiency and reliability, the plant design and development must be optimized [9-11]. Plant architecture and layout should fit the application type, considering packaging and weight constraints. In fact, while for trucks, off-road engines, power generation engines, as well as marine engines, it is convenient to consider solutions to exploit the low temperature heat sources to preheat the working fluid before entering the evaporator [12], simple configurations are usually more appropriate for passenger cars [13]. Fitting an ORC system on the exhaust line of an engine increases the weight and complexity of the overall system and the exhaust gas backpressure, which could lead to performance degradation. The engine backpressure can be counter-balanced implementing appropriate turbocharging strategies, choosing for example a Variable Geometry Turbine (VGT). Such solution would help in limiting the negative effect of the increased back pressure caused by the exhaust gas heat exchanger. In fact, it has been demonstrated by means of numerical simulations that, adopting a VGT, the engine brake specific fuel consumption is only weakly affected by the ORC system if the backpressure increase is below 100 mbar [13].

The choice of the ORC working fluid plays a very important role, being decisive for cycle efficiency, environmental impact, and system safety. From a thermodynamic point of view, the fluids are classified depending on the slope of the saturation vapor curve in the Temperature-Entropy (T-s) diagram: fluids with a positive slope are called “dry”, those with a negative slope “wet”, and fluids having a nearly vertical saturation curve “isentropic”. Isentropic or dry fluids are preferred in Rankine Cycles to avoid the presence of liquid droplets during the expansion. However, a dry fluid can leave the expander with substantial unrecovered heat, which is consequently wasted, also increasing the cooling load in the condenser. Eventually, such heat can be used to preheat the fluid at the pump outlet before it enters the boiler. Wet fluids, on the other hand, will need higher turbine inlet temperature to avoid the two-phase region [14]. Latent heat, density and specific heat are also important properties to be considered in choosing the optimal ORC working fluid. Some studies demonstrated that fluids with high latent heat, high density and low liquid specific heat are preferable as they can absorb more energy from the source in the evaporator, hence requiring low working fluid mass flow rate. Consequently, the size of the system components is reduced, as well as the work absorbed by the pump [15]. Another important thermodynamic property is the freezing point of the fluid, which must be below the lowest operating temperature in the cycle. The fluid must also work in an acceptable pressure range, avoiding too high pressure or high vacuum, which would impact the cost of the system.

Concerning safety and environment, fluids are classified according to the National Fire Protection Association (NFPA) 704 Standard [16]. The working fluids are categorized based on their health, flammability, and chemical instability-reactivity hazards. The working fluid must also have a low global warming potential (GWP): this is a measure of

how much energy the emissions of 1 ton of a gas will absorb over a given period of time, relative to the emissions of 1 ton of carbon dioxide (CO2). The larger the GWP, the more a given gas warms the Earth compared to CO2 over that time period [17].

In ORC systems, the energy can be recovered from many heat sources at different temperatures. Exhaust gases are classified as high-temperature heat sources, with values ranging between 200 and 600 °C, while coolant (80–100 °C), lube oil (80–120 °C) and the charge air cooling (CAC, 30–50 °C) are considered low temperature heat sources [15]. Temperature values depend on the engine operating point. In engine waste heat recovery systems, exhaust gas and recycled exhaust gases are commonly exploited due to their high temperature. Conversely, engine coolant, CAC and lube oil heat recovery are less common in the literature because of the lower temperature and potential, despite the exploitation of such waste heat could be beneficial for the vehicle thermal management [18]. Usually alcohols (e.g., ethanol, methanol), water steam and hydrocarbons (e.g., benzene, toluene, pentane, octane, cyclohexane, and cyclopentane) are suitable for waste heat recovery from high temperature heat sources, even though some of them display flammability concerns. Mixtures of alcohols with water have also been considered to decrease flammability issues. Refrigerants are usually more suitable for low temperature waste heat recovery, such as CAC and coolant.

The hot stream undergoes a large temperature change in the heat exchanger with an important exergy destruction related to the temperature difference between the fluids in the same component. Using mixtures instead of pure fluids as a working fluid allows variable temperature heat transfer, reducing the temperature difference between hot and cold streams, which in turn reduces the exergy destruction in the thermodynamic cycle [19, 20]. However, the screening process for the determination of mixture components and their fractions is very complex and more research is required for the adoption of such solutions [21].

ORC bottoming engines must also adopt an appropriate condensing strategy. There are some possibilities for engine waste heat recovery in vehicle applications: indirect condensation using the engine cooling circuit as heat sink (temperature range around 80–100 °C), indirect condensation using a lower temperature cooling circuit (e.g., CAC, temperature 30–50 °C), or direct cooling using an ambient air condenser (installed in the vehicle cooling pack). In the first two cases, the coolant heat must also be rejected to the environment through the vehicle cooling package. Condensing temperature depends on expected ambient conditions. In marine and stationary applications, there are fewer constraints affecting the condenser installation, and the availability of a cooling medium such as sea or fresh water.

This paper presents the results of a numerical analysis proposing an ORC system bottoming a natural gas spark ignition engine powering a bus, using experimental data obtained from road tests. The aim is the estimation of the recoverable mechanical power and the consequent engine efficiency increase. The available thermal power for the ORC system was measured on the vehicle performing a driving cycle in real conditions. Exhaust gas mass flow rate and temperature were recorded together with engine rotational speed and instantaneous torque. A ten-point grid in the torque-speed plane was used for grouping the engine operating conditions, each node being characterized by a residence time, exhaust mass flow rate and temperature values. The actual Rankine cycle was calculated considering the grid node conditions, obtaining the recovered power and the engine efficiency increase. N-pentane (R601) was chosen as working fluid for the ORC simulations.

2 Modelling and analysis

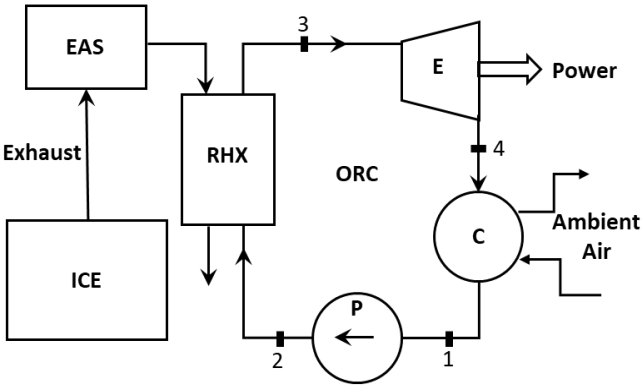

Fig.1. Sketch of the ORC system.

Figure 1 shows the ORC system considered in the paper. The use of regeneration has not been considered for sake of simplicity. The main engine characteristics are reported in Table 1. The speed profile recorded during the test is reported in Figure 2.

Table 1. Engine and vehicle main characteristics.

Engine type	4-stroke turbocharged SI
Displacement	7.8 l
Cylinders	6 in line
Rated torque	1300 Nm @ 1200 rpm
Rated power	243 kW @ 2000 rpm
Bore	115 mm
Stroke	125 mm
Compression ratio	11:1
Fuel	Natural Gas

Realistic engine operating conditions and the corresponding exhaust gas conditions have been considered for the numerical simulation since the vehicle performed road tests, whose speed profile is reported in Figure 2.

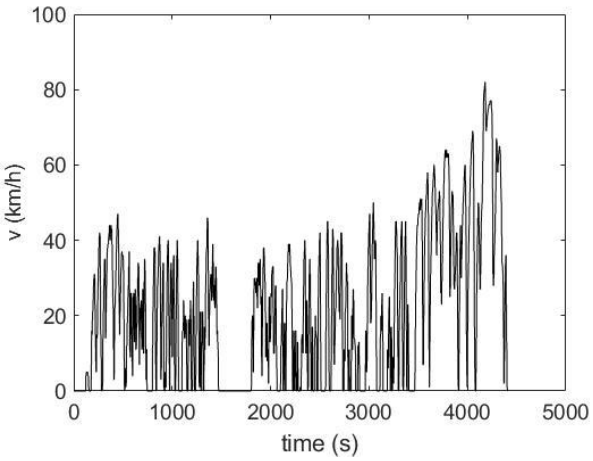

Fig. 2. Instantaneous vehicle speed measured over the driving cycle.

Engine speed, torque, fuel mass flow rates and exhaust gas temperature have been sampled during the road test from the engine control unit (ECU) with a frequency of 1 Hz. The engine operating conditions on the torque-engine speed plane are reported in Figure 3. The engine mainly operated at low speed over the test, while engine torque varied between part and full load operating conditions.

A reduced number of exhaust gas mass flow rate and temperature conditions have been selected as input for ORC calculations by using a 10-point grid on the torque-speed plane including idle operation, Figure 4. A generic operating condition is attributed to the closest grid point and the residence time evaluated considering an inverse proportionality to its distance from the grid points. The assignment criterion imposes that the work of the engine operating point equals the sum of work of the adjacent grid points [22]. The residence time at each node of the grid is proportional to the bubble area. The effects of load transient on fuel consumption have been neglected. Table 2 displays the residence time as percent of the total road test duration.

Table 2. Engine speed (n), torque (T_{eng}), percent residence time (τ), exhaust gas temperature (T_{ex}) and mass flow rate (mfr_{ex}) for each grid point.

Grid point	n (rpm)	T_{eng} (N m)	τ (%)	T_{ex} (°C)	mfr_{ex} (kg h^{-1})
1	600	0	37.41	329	10.3
2	900	150	8.41	373	68.5
3	900	500	9.11	393	176.5
4	900	850	3.28	418	284.5
5	1250	150	8.47	413	102.5
6	1250	500	12.83	435	246.0
7	1250	850	5.30	456	389.5
8	1600	150	4.36	462	155.5
9	1600	500	7.91	483	350.0
10	1600	850	2.92	494	544.4

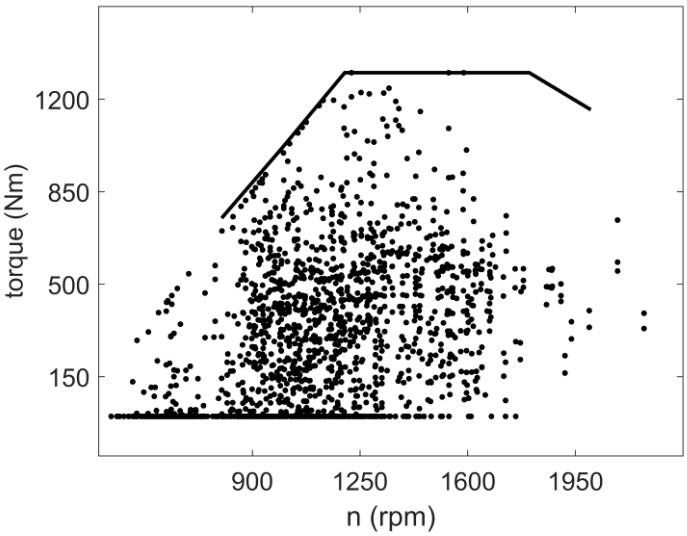

Fig. 3. Engine operating points over the driving cycle.

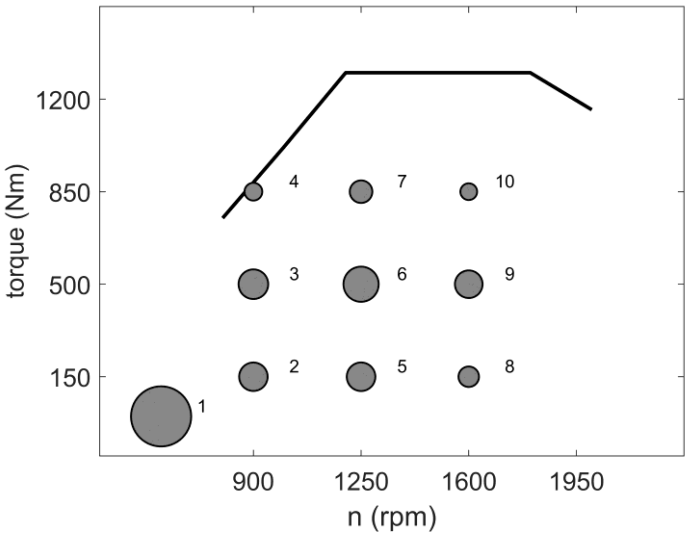

Fig. 4. Engine torque curve and discretization grid. Bubble area proportional to the residence time.

In the present study, the working fluid employed is n-pentane (R601) which is a hydrocarbon belonging to the dry fluid class. Dry fluids are preferable for direct cycles because an isentropic expansion, starting at saturated vapor conditions, ends in the superheated vapor zone [23]. However, fluids belonging to the dry class would exit the expander with considerable residual enthalpy.

R601 has a critical temperature of 469.7 K and a critical pressure of 33.7 bar [24]. At atmospheric pressure, the saturation temperature is 309.1 K and the enthalpy of evaporation is equal to 357.7 kJ kg^{-1}.

NFPA 704 standards consider R601 flammability high while its health hazard is low and no chemical instability is observed; it does not have Ozone Depletion Potential while the 100 years Global Warming Potential is 5 [8, 25]. The working fluid selection is a compromise among different characteristics. R601 has been selected as working fluid as its thermodynamic properties are very well suitable for the specific application.

In addition to the ORC fluid, the expander selection is also very important for ORC systems because its performance strongly affects the actual cycle efficiency. In this case, considering the ORC system characteristics, a positive displacement expander has been selected. According to the literature, 0.70 was considered as the isentropic efficiency of the expander [26], while the pump efficiency was fixed equal to 0.65 [27, 28].

Pressure losses in pipes and heat exchangers have been neglected in the Rankine cycle calculations. In particular, the effect of the exhaust backpressure on engine efficiency caused by the recovery heat exchanger (RHX) has been neglected, in accordance with other authors [29]. The effect of the ORC system mass has not been considered when modelling the vehicle dynamic, assuming that it can be in a first approximation neglected in comparison with the vehicle mass.

The working fluid mass flow rate was determined imposing a totally evaporated stream at the RHX exit, limiting the maximum cycle temperature at 469.7 K, which is the critical temperature for n-Pentane. The heat exchanger was assumed to be crossflow with an overall conductance ($U \cdot A$) equal to 75 W/K.

DWSIM is used to perform Rankine cycle simulations [30, 31]. The software, a process simulator, is capable of modelling phase equilibria covering a variety of systems. It can model phase equilibria between solids, vapor and up to two liquid phase mixtures. Fluid

properties were calculated using CoolProp [32], while the fluid phase change was modelled using the Nested Loop flash algorithm [31]. The program contains different components like pumps, turbines, heat exchangers which can be implemented with different solver options.

3 Results

This section presents the results of the numerical simulations showing ORC performance in terms of optimized operating conditions, net power output and cycle efficiency. The overall impact of the bottoming ORC device on vehicle fuel consumption over the road test is also determined.

The operating condition with the highest exhaust energy is grid node number 6, Table 2, with 246 kg h^{-1} engine exhaust mass flow rate and 708 K temperature. This point is considered for showing the effects of the Rankine cycle design parameters on system performance.

The condensation temperature is set to 319 K, because it has been assumed that the cold fluid, air, enters the condenser at 298 K and imposing a minimum temperature difference between the fluids of 21 K [33], Table 3. The maximum ORC pressure was varied between 10 and 30 bar to show the effect on cycle efficiency.

Table 3 Cycle temperatures and pressures

T_1 [K]	P_1 [bar]	P_2 [bar]	T_3 [K]
319	1.4	10 - 30	$< T_c$

The actual Rankine cycle for R601 is represented in Figure 5 in a T-s plane. The thermodynamic performance of the cycle depends on the temperatures at which the thermal power is adduced to and subtracted from the working fluid. The maximum cycle temperature is limited by the exhaust gas temperature and the condensation pressure is constrained by the temperature of the air entering the condenser. Belonging R601 to the dry-fluid class, it exits the expander with a large residual enthalpy which could be exploited using a regenerative cycle but to keep the system simple, no regeneration has been considered in this paper. In fact, the R601 fluid crosses the isobar at which condensation takes places with a quite high temperature and far from the saturation curve, thus increasing the mean temperature of heat rejection and reducing the cycle efficiency.

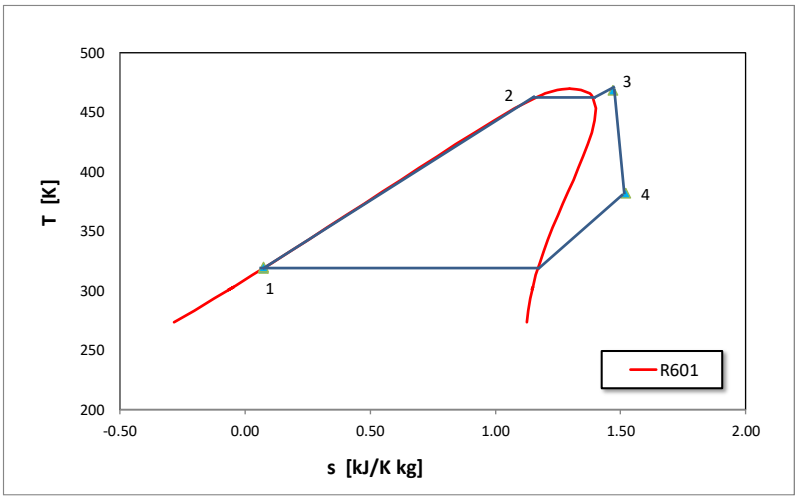

Fig. 5. Actual Rankine cycle in the Temperature-entropy diagram.

Depending on the available exhaust heat, an appropriate working fluid mass flow rate should be processed to guarantee a fully evaporated fluid entering the expander. The maximum ORC temperature, indicated with T_3, consequently depends on the available thermal power, on the maximum cycle pressure and on the working fluid mass flow rate, Figure 6. In this analysis T_3 was kept below 469.7 K, the fluid critical temperature. Maximum cycle temperature T_3 reduces with increasing ORC mass flow rate and, in addition, as the maximum pressure increases the usable ORC mass flow rate change shrinks.

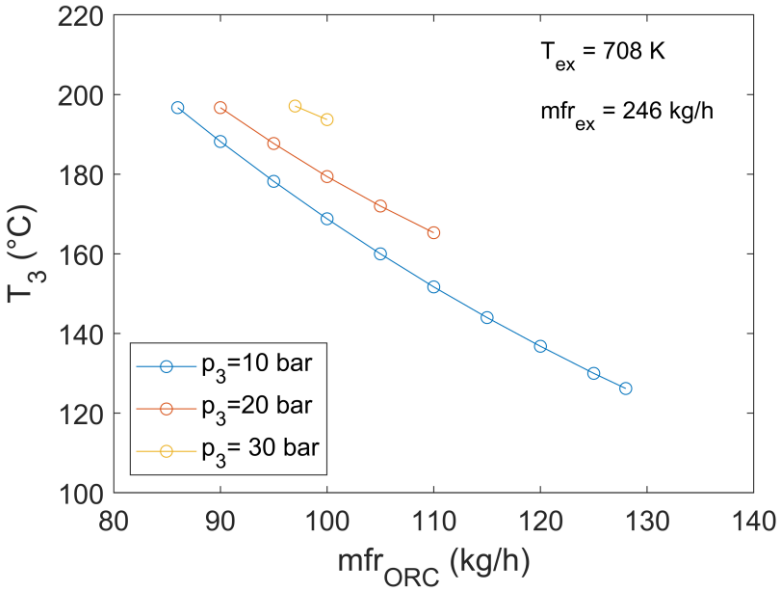

Fig. 6. ORC maximum cycle temperature as a function of working fluid mass flow rate at different maximum cycle pressures, grid point 6.

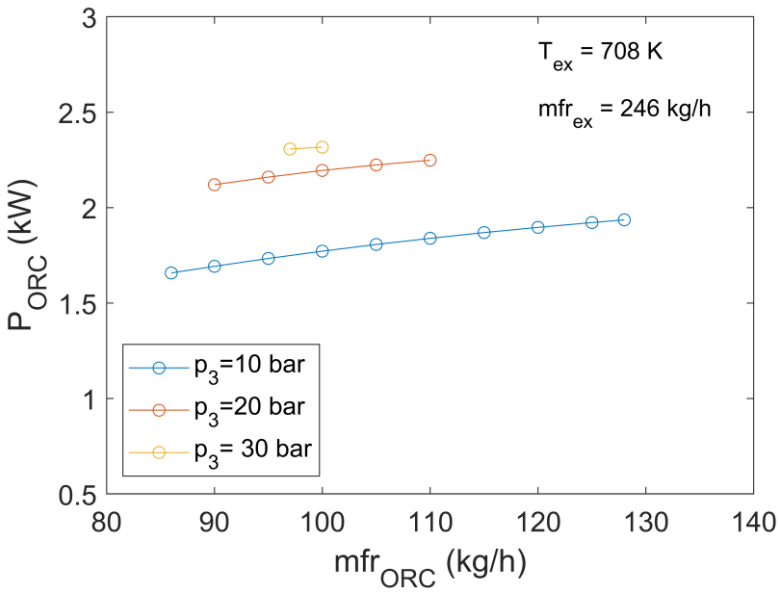

Fig.7. ORC power as a function of the working fluid mass flow rate at different maximum cycle pressures, grid point 6.

The influence of the maximum cycle pressure p_3 and mass flow rate on the ORC power P_{ORC} is displayed in Figure 7 for the engine operating condition of grid point 6. Low pressure levels allow a wider range of possible working fluid mass flow rates, but the delivered power is small due to low average heat adduction temperature. As the pressure increases so does also the power output for a fixed mass flow rate. The trend becomes less evident as the pressure p_3 approaches the critical pressure. For each pressure level, the lowest mass flow rate in the plots of Figure 7 is determined imposing a maximum temperature T_3 lower than the critical temperature. The highest mass flow rate is the maximum flow rate which can be vaporized in the RHX.

Figure 8 shows the effect of maximum cycle pressure p_3 on the ORC power and thermodynamic cycle efficiency. As expected, ORC delivered power shows a growing trend with p_3, which is however a design parameter requiring attention as it must match the exhaust gas conditions, i.e. hot fluid inlet temperature. For the operating conditions of Figure 8, exhaust gas temperature and mass flow rate are 708 K and 246 kg h^{-1}, represented by the node number 6 of the discretization grid. At such conditions, it was possible to fully vaporize an ORC working fluid mass flow rate of 100 kg h^{-1} up to 30 bar maximum pressure. The ORC power ranges between 1.8 kW at p_3=10 bar and 2.3 kW at p_3=30 bar with an ORC cycle efficiency between 11% and 15%.

The ORC performance over the road test have been evaluated considering the heat recovered from the exhaust gases in the operating conditions corresponding to each grid node, the working fluid maximum pressure being 30 bar. The available exhaust heat depends on the engine operating conditions. At higher engine loads and speeds, the exhaust mass flow rate and temperature increase, and consequently the ORC delivers more power, Figure 9, with values between 0.13 kW at idle and 3.1 kW at node 10, and a cycle efficiency of 15 %. ORC efficiency is constant because p_3 is 30 bar for all grid nodes and T_3 varies in a small range between 462 K, the saturation temperature of R601 at 30 bar, and 469.7 K, its critical temperature. The working fluid mass flow rate has been modified depending on the p_3 value for attaining a complete vaporization of R601 into the RHX.

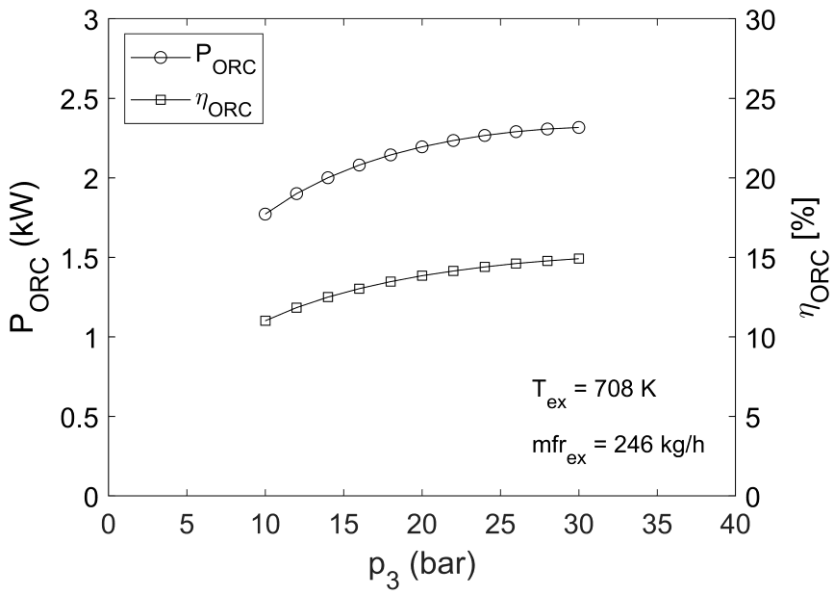

Fig.8. ORC power and thermodynamic cycle efficiency as a function of the maximum cycle pressure, grid point 6.

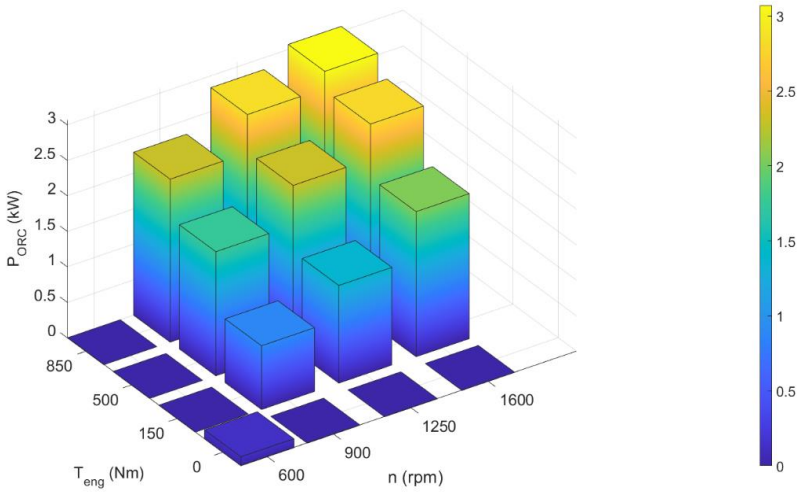

Fig.9. ORC delivered power at the engine operating points of the discretization grid.

For a hybrid powertrain configuration, the ORC power can contribute to vehicle propulsion or to power auxiliary devices. Knowing the fuel mass flow rate for each operating condition and comparing the engine power with the ORC power at each grid node, it is possible to calculate the fuel saving according to the following equation (1):

$$\Delta mfr_{fuel} = \frac{P_{ORC}}{P_{eng}} \cdot 100 \quad (1)$$

At idle, the fuel consumption reduction was estimated assuming a friction mean effective pressure of 0.80 bar. The effects of engine transient on fuel consumption and ORC thermodynamic cycle have been neglected.

Fuel consumption reduction is displayed for all grid nodes in Figure 10, with values between 2.2% for node 10 and 8.1% for node 8. In fact, part load operation is characterized by a higher ratio between exhaust and engine power, therefore higher fuel saving results for this condition.

By considering the percent residence time, the total test duration and the fuel mass flow rates at each discretized operating condition, a total fuel consumption of 6727 g of natural gas was estimated. Being 24.78 km the length of the road test, the consumption was 271.5 g/km. Considering the power recovered from the ORC, according to the adopted assumptions, the fuel consumption could be reduced to 261.4 g/km, corresponding to a 3.7% fuel saving.

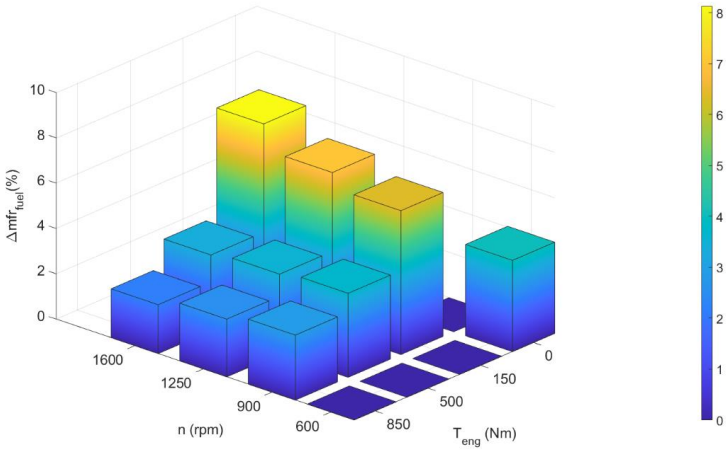

Fig.10. Fuel consumption reduction at the engine operating points of the discretization grid.

Summary

A bus powered by a natural gas spark ignition engine has been tested in real driving conditions. The engine exhaust gases were then considered as thermal heat source into a recovery heat exchanger, for vaporizing the working fluid of an Organic Rankine Cycle.

The calculations have been accomplished considering n-pentane (R601) as working fluid. To reduce the number of exhaust gas conditions for simulating the ORC performance, engine torque-speed values determined over the road test were discretized using a grid of 10 nodes into the engine torque-speed plane, each node characterized by a residence time. The discretization process has been required for considering a reduced number of exhaust gas conditions as input for the ORC analysis.

Numerical simulations have shown that the ORC delivered power increases with the engine load and speed since the exhaust mass flow rate and temperature are high. The ORC power ranges between 0.13 at idle and 3.1 kW at node 10. The Rankine cycle efficiency is constant at all grid node points with values of 15% since the ORC maximum cycle pressure and temperature do not change for all grid points.

In a vehicle with a hybrid powertrain configuration, the ORC power could contribute to vehicle propulsion or to power auxiliary devices, with a fuel saving ranging between 2.2%

for the node 10 and 8.1% for the node 8. In fact, part load operations are characterized by a higher ratio between exhaust and engine power, the fuel saving resulting higher for such conditions.

The ORC recovered power could allow a reduction of the fuel consumption over the road test from 271.5 g/km to 261.4 g/km, corresponding to a 3.7% fuel saving.

The ORC system is then a promising solution for increasing the efficiency of internal combustion engines in large vehicles such as buses and trucks, where the installation of the bottoming ORC system is possible with manageable integration issues.

References

[1] United Nations, Kyoto protocol to the united nations framework convention on climate change, (1998). https://unfccc.int/resource/docs/convkp/kpeng.pdf.

[2] Eurostat, Complete energy balances, (2020). nrg_bal_c (accessed April 30, 2020).

[3] T. Dyr, P. Misiurski, K. Ziółkowska, Costs and benefits of using buses fuelled by natural gas in public transport, J. Clean. Prod. 225 (2019) 1134–1146. https://doi.org/10.1016/j.jclepro.2019.03.317.

[4] T.L.F. Brito, E. Moutinho dos Santos, R. Galbieri, H.K. de M. Costa, Qualitative Comparative Analysis of cities that introduced compressed natural gas to their urban bus fleet, Renew. Sustain. Energy Rev. 71 (2017) 502–508. https://doi.org/10.1016/j.rser.2016.12.077.

[5] J. Heywood, Internal combustion engine fundamentals, Mc Graw-Hill, New York, 1989.

[6] M. Stuhldreher, J. Kargul, D. Barba, J. McDonald, S. Bohac, P. Dekraker, A. Moskalik, Benchmarking a 2016 Honda Civic 1.5-Liter L15B7 Turbocharged Engine and Evaluating the Future Efficiency Potential of Turbocharged Engines, SAE Int. J. Engines. 11 (2018) 1273–1305. https://doi.org/10.4271/2018-01-0319.

[7] S. Lion, C.N. Michos, I. Vlaskos, R. Taccani, A thermodynamic feasibility study of an Organic Rankine Cycle (ORC) for heavy-duty diesel engine waste heat recovery in off-highway applications, Int. J. Energy Environ. Eng. 8 (2017) 81–98. https://doi.org/10.1007/s40095-017-0234-8.

[8] S. Lion, C.N. Michos, I. Vlaskos, C. Rouaud, R. Taccani, A review of waste heat recovery and Organic Rankine Cycles (ORC) in on-off highway vehicle Heavy Duty Diesel Engine applications, Renew. Sustain. Energy Rev. 79 (2017) 691–708. https://doi.org/10.1016/j.rser.2017.05.082.

[9] Y. Dai, J. Wang, L. Gao, Parametric optimization and comparative study of organic Rankine cycle (ORC) for low grade waste heat recovery, Energy Convers. Manag. 50 (2009) 576–582. https://doi.org/10.1016/j.enconman.2008.10.018.

[10] B. Xu, D. Rathod, A. Yebi, Z. Filipi, A comparative analysis of real-time power optimization for organic Rankine cycle waste heat recovery systems, Appl. Therm. Eng. 164 (2020) 114442. https://doi.org/10.1016/J.APPLTHERMALENG.2019.114442.

[11] N. Nazari, P. Heidarnejad, S. Porkhial, Multi-objective optimization of a combined steam-organic Rankine cycle based on exergy and exergo-economic analysis for waste heat recovery application, Energy Convers. Manag. 127 (2016) 366–379. https://doi.org/10.1016/j.enconman.2016.09.022.

[12] G. Valencia, A. Fontalvo, Y. Cárdenas, J. Duarte, C. Isaza, Energy and exergy analysis of different exhaust waste heat recovery systems for natural gas engine based on ORC, Energies. 12 (2019). https://doi.org/10.3390/en12122378.

[13] C.N. Michos, S. Lion, I. Vlaskos, R. Taccani, Analysis of the backpressure effect of an Organic Rankine Cycle (ORC) evaporator on the exhaust line of a turbocharged

heavy duty diesel power generator for marine applications, Energy Convers. Manag. 132 (2017) 347–360. https://doi.org/10.1016/j.enconman.2016.11.025.

[14] H. Chen, D.Y. Goswami, E.K. Stefanakos, A review of thermodynamic cycles and working fluids for the conversion of low-grade heat, Renew. Sustain. Energy Rev. 14 (2010) 3059–3067. https://doi.org/10.1016/j.rser.2010.07.006.

[15] V. Maizza, A. Maizza, Unconventional working fluids in organic Rankine-cycles for waste energy recovery systems, Appl. Therm. Eng. 21 (2001) 381–390. https://doi.org/10.1016/S1359-4311(00)00044-2.

[16] NFPA, https://www.nfpa.org/, (n.d.). https://www.nfpa.org/ (accessed August 28, 2019).

[17] EPA, Greenhouse Gas Emissions, (n.d.). https://www.epa.gov/ghgemissions/understanding-global-warming-potentials] (accessed September 30, 2019).

[18] W.K. Dimitrios T. Hountalas, Georgios C. Mavropoulos, Christos Katsanos, Improvement of bottoming cycle efficiency and heat rejection for HD truck applications by utilization of EGR and CAC heat, Energy Convers. Manag. 53 (2012) 19–32. https://doi.org/10.1016/j.enconman.2011.08.002.

[19] Y.J. Baik, M. Kim, K.C. Chang, Y.S. Lee, H.K. Yoon, Power enhancement potential of a mixture transcritical cycle for a low-temperature geothermal power generation, Energy. 47 (2012) 70–76. https://doi.org/10.1016/j.energy.2012.06.041.

[20] M. Chys, M. van den Broek, B. Vanslambrouck, M. De Paepe, Potential of zeotropic mixtures as working fluids in organic Rankine cycles, Energy. 44 (2012) 623–632. https://doi.org/10.1016/j.energy.2012.05.030.

[21] R. Scaccabarozzi, M. Tavano, C.M. Invernizzi, E. Martelli, Thermodynamic Optimization of heat recovery ORCs for heavy duty Internal Combustion Engine: Pure fluids vs. zeotropic mixtures, Energy Procedia. 129 (2017) 168–175. https://doi.org/10.1016/j.egypro.2017.09.099.

[22] A. Mariani, B. Morrone, A. Unich, Numerical evaluation of internal combustion spark ignition engines performance fuelled with hydrogen – Natural gas blends, Int. J. Hydrogen Energy. 37 (2012) 2644–2654. https://doi.org/10.1016/j.ijhydene.2011.10.082.

[23] C. He, C. Liu, H. Gao, H. Xie, Y. Li, S. Wu, J. Xu, The optimal evaporation temperature and working fluids for subcritical organic Rankine cycle, Energy. 38 (2012) 136–143. https://doi.org/10.1016/j.energy.2011.12.022.

[24] J. Bao, L. Zhao, A review of working fluid and expander selections for organic Rankine cycle, Renew. Sustain. Energy Rev. 24 (2013) 325–342. https://doi.org/10.1016/j.rser.2013.03.040.

[25] ASHRAE, Update on New Refrigerants Designations and Safety Classifications, (2015) 1–4. https://www.ashrae.org/technical-resources/standards-and-guidelines/ashrae-refrigerant-designations (accessed November 12, 2019).

[26] Y. Glavatskaya, P. Podevin, V. Lemort, O. Shonda, G. Descombes, Reciprocating expander for an exhaust heat recovery rankine cycle for a passenger car application, Energies. 5 (2012) 1751–1765. https://doi.org/10.3390/en5061751.

[27] R. Mastrullo, A.W. Mauro, R. Revellin, L. Viscito, Modeling and optimization of a shell and louvered fin mini-tubes heat exchanger in an ORC powered by an internal combustion engine, Energy Convers. Manag. 101 (2015) 697–712. https://doi.org/10.1016/j.enconman.2015.06.012.

[28] S. Declaye, S. Quoilin, L. Guillaume, V. Lemort, Experimental study on an open-drive scroll expander integrated into an ORC (Organic Rankine Cycle) system with R245fa as working fluid, Energy. 55 (2013) 173–183. https://doi.org/10.1016/j.energy.2013.04.003.

[29] C.O. Katsanos, D.T. Hountalas, E.G. Pariotis, Thermodynamic analysis of a Rankine cycle applied on a diesel truck engine using steam and organic medium, Energy Convers. Manag. 60 (2012) 68–76. https://doi.org/10.1016/j.enconman.2011.12.026.
[30] M. Leino, Process Simulation Unit Operation Models – Review of Open And Hsc Chemistry I / O Interfaces, Tampere University of Technology, 2016. https://trepo.tuni.fi//handle/123456789/23943.
[31] DWSIM, (2015). http://dwsim.inforside.com.br/wiki/index.php?title=DWSIM (accessed November 12, 2019).
[32] I.H. Bell, J. Wronski, S. Quoilin, V. Lemort, Pure and pseudo-pure fluid thermophysical property evaluation and the open-source thermophysical property library coolprop, Ind. Eng. Chem. Res. 53 (2014) 2498–2508. https://doi.org/10.1021/ie4033999.
[33] J. Lin, A.J. Mahvi, T.S. Kunke, S. Garimella, Improving air-side heat transfer performance in air-cooled power plant condensers, Appl. Therm. Eng. 170 (2020) 114913. https://doi.org/10.1016/j.applthermaleng.2020.114913.

Nomenclature

A	Area [m^2]
C	Condenser
E	Expander
EAS	Exhaust After-treatment system
ECU	Engine Control Unit
ICE	Internal Combustion Engine
M	Mass [kg]
mfr	Mass flow rate [kg/h]
N	Engine speed [RPM]
ORC	Organic Rankine Cycle
p	Pressure [bar]
P	Power [kW], Pump
RHX	Recovery Heat Exchanger
R601	n-Pentane
s	Entropy [kJ/kgK]
T	Temperature [K], Torque [Nm]
U	Overall heat transfer coefficient [$W\ m^{-2}\ K^{-1}$]
v	Speed [km/h]
Subscripts	
eng	Engine
ex	Exhaust gases
Greek symbols	
η	Efficiency [-]
Δ	Variation
τ	Residence time [-]